Check for updates

ADVANCED ENGINEERING MATERIALS
www.aem-journal.com

Enhancement of Damping Characteristics through Hybridization: Investigating the Synergistic Effects of Triply Periodic Minimal Surface Additive Metals and Silicone Polymers

*Murat Can Ozden, Ugur Simsek, Mirhan Ozdemir, Cemal Efe Gayir, and Polat Sendur**

Using triply periodic minimal surface (TPMS) metal parts with added silicone polymer can lead to the development of hybrid materials with enhanced damping characteristics. This study aims to develop composite structures by hybridizing additively manufactured TPMS metal parts with added silicone polymers for vibration applications. Central to this investigation is the quest to ascertain the most efficacious damping mechanism. In this context, the finite element method (FEM)-based model of the primitive TPMS structure, consisting of cobalt–chrome (CoCr) and the concomitant hybrid structure integrated with silicone polymer, is meticulously developed. The damping characteristics of the FEM-based models are obtained by modal analysis. The models are also validated using experimental modal tests. The findings show a significant improvement in damping characteristics thanks to the hybrid TPMS structure. Specifically, the damping ratios derived from the hybrid TPMS structure exhibit a sixfold increase in time-domain damping and up to a 30-fold increase in frequency-based analysis across two distinct damping calculation methodologies. Overall, this study highlights the potential of additively fabricated primitive TPMS metal parts with added silicone polymer as a promising structure for improving damping properties in various engineering applications.

1. Introduction

Additive manufacturing of triply periodic minimal surface (TPMS) structures has gained significant attention in recent years due to their unique and desirable structural and mechanical properties. TPMS structures can minimize surface area while maintaining a repeating pattern in 3D, leading to a high strength-to-weight ratio, stiffness, and other favorable mechanical properties. This has made TPMS structures a promising candidate for various mechanical applications in the future.[1]

Obtaining optimal damping behavior is a crucial aspect in engineering applications; however, it can also be challenging due to the trade-offs between the stiffness and damping properties of systems, fatigue, durability, and cost considerations. Although there are many optimization studies aimed at improving the TPMS structures' stiffness properties, the literature on damping characterization of these structures is limited. Studies on the characterization and optimization of damping in TMPS structures and metamaterials continue actively, as in many current engineering topics. In actively ongoing studies conducted on damping properties of metamaterials, the effects of changes in lattice type on the damping characteristics are investigated,[2–4] as well as the effects of volumetric density[5–7] and the benefits of using multi-material layer structures.[8–10]

Polymers are preferred materials in many engineering applications that require damping performance due to their unique mechanical properties and absorption characteristics thanks to their atomic structures. Polymers, with their distinctive capabilities such as low elastic modulus values and high damping capacities, can provide engineering structures with desired capabilities to engineering systems, such as reduction of vibration amplitude and energy absorption under dynamic loads for stable performance in engineering systems.[11] Silicone, a member of this material family, stands out from other members of the material family with its high-temperature resistance, oxidation resistance, chemical resistance, and high elasticity properties. Its high

M. C. Ozden
Mechanical Engineering Department
Ozyegin University
Istanbul 34794, Turkey

U. Simsek, M. Ozdemir, C. E. Gayir, P. Sendur
Vibrations and Acoustics Laboratory
Ozyegin University
Istanbul 34794, Turkey
E-mail: polat.sendur@ozyegin.edu.tr

The ORCID identification number(s) for the author(s) of this article can be found under https://doi.org/10.1002/adem.202302181.

© 2024 The Authors. Advanced Engineering Materials published by Wiley-VCH GmbH. This is an open access article under the terms of the Creative Commons Attribution-NonCommercial-NoDerivs License, which permits use and distribution in any medium, provided the original work is properly cited, the use is non-commercial and no modifications or adaptations are made.

DOI: 10.1002/adem.202302181

15272648, 2024, 11, Downloaded from https://advanced.onlinelibrary.wiley.com/doi/10.1002/adem.202302181 by Ozyegin University, Wiley Online Library on [25/06/2025]. See the Terms and Conditions (https://onlinelibrary.wiley.com/terms-and-conditions) on Wiley Online Library for rules of use; OA articles are governed by the applicable Creative Commons License

damping capacity makes it a good damping system element for many engineering systems.[12–14]

To achieve superior performance, the unique damping properties of polymer materials are combined with the desired engineering properties of other materials and used in various hybrid structures by combining them.[15,16] Interpenetrating phase composite (IPC) materials, which have been the subject of much research in recent years, are examples of such hybrid structures. In this composite approach, materials consisting of two or more interpenetrating phases occupy the same volume. The phases of these materials are continuous and interconnected, and they can consist of different materials with different properties.[17] The properties of IPC materials have been investigated from many engineering perspectives. In particular, the rigidity,[18] energy absorption capacity,[19,20] and elastic properties[21] brought about by the hybrid structure have been examined in the literature.

Although numerous studies have considered the damping properties of polymers within hybrid configurations, the literature lacks exploration into hybrid structures integrating TPMS metal components with silicone polymers to enhance vibration and damping characteristics. This study fills this gap by providing insights into the use of primitive TPMS components with silicone polymers to create novel materials with superior damping properties specifically designed for vibration applications.

Using finite element method (FEM) modeling, this research highlights the impact of polymer incorporation on damping behavior, natural frequencies, and damping capacities over a wide frequency range within the hybrid structure. Furthermore, the modeling approach is validated with experimental modal testing. This study aims to achieve a substantial enhancement in damping properties with the introduction of silicone polymer into TPMS metal components, thus underlining the potential of this hybrid structure as a promising material for improved damping attributes in diverse engineering applications.

The remainder of the article is organized as follows: design of TPMS structures in Section 2.1, FEM modeling in Section 2.2, polymer material selection in Section 2.3, different damping characterization methods in Section 2.4, FEM analysis in Section 3.1, manufacturing of test specimen in Section 3.2, and modal test methodology and validation in Section 3.3. These are further discussed in Section 4, leading to the conclusions presented in Section 5.

2. Experimental Section

2.1. Design of TPMS Structures

In this study, the primitive structure, a unique member of the surface-based TPMS family, was used as a base material for fabricating a novel composite structure with enhanced damping properties. TPMS structures are unique geometric structures that exhibit a high degree of symmetry and are defined by the mathematical relationship between two interpenetrating periodic lattices. There are numerous types of TPMS structures with different symmetries, shapes, and sizes, each with unique properties and potential applications. In this study, we used primitive structures as the fundamental building blocks for our composite material due to their simplicity and ease of fabrication. However, the methodology presented is also applicable to other TPMS structures.

The mathematical expressions of TPMS structures are complex and variable. However, TPMS structures are generally created by assembling 2D layers sequentially, and their mathematical expressions are usually represented as Fourier series.[22] The coefficients expressing these series can also be used to control TPMS topologies and their mechanical properties. The surface function equations that represent the explicit mathematical expressions of surface-based primitive lattice structure are given in Equation (1).

$$U_{\mathrm{P}}(x, y, z, t) = (\cos(k_{\mathrm{x}}x) + \cos(k_{\mathrm{y}}y) + \cos(k_{\mathrm{z}}z))^2 - t^2 \tag{1}$$

where t is level-set parameter to control the offset value from the isosurface $U = 0$. k_{i} ($i = x, y, z$) terms represent the periodicity of the TPMS structures in x, y, and z-directions as given in Equation (2).

$$k_{\mathrm{i}} = 2\pi \frac{n_{\mathrm{i}}}{l_{\mathrm{i}}} \tag{2}$$

where n_{i} and l_{i} are the number of lattices and absolute size of the structure in x, y, and z directions. In this study, a primitive structure with a relative density, ρ^*, of 0.2 was used. The isosurface, unit cell with relative density $\rho^* = 0.2$, and fabricated structure are presented in **Figure 1**a–c, respectively.

A test specimen geometry was proposed to demonstrate and quantify the enhancement in the damping performance of the proposed composite structure (see Figure 1c). The $36 \times 36 \times 216$ mm test specimen, consisting of primitive unit cells with a 12 mm unit-cell size, was sandwiched between 1 mm-thick metallic plates. The void volume in the metallic core was then filled with a polymeric material.

2.2. Finite-Element Method Modeling

FEM was used as the numerical analysis method in this study. A set of finite-element analyses was performed to characterize the dynamic performance of the proposed test specimen. The dimensions of the test specimen and FEM model details are given in **Figure 2**. To construct the model, the lattice core was first modeled with voxel elements using a MATLAB script. The advantages of voxel modeling for such lattice structures were reported in the literature regarding the applicability and computational efficiency of different modeling techniques.[23] Besides, as suggested in the same study, the number of elements throughout the thickness was determined by performing a mesh convergence analysis. Similarly, the polymeric volume was modeled with voxel elements for a consistent mesh. Finally, the plates were modeled with shell elements assigning proper section properties to represent the plate thickness. The FEM models of metal-only and hybrid structures consisted of 750 K and 3.6 M elements, respectively. Modeling of the hybrid structure was carried out by considering that the nodes of both structures were rigidly connected to each other. Therefore, in modeling the hybrid structure, the nodes of the metal and polymer structures were connected node to node. This assumption was made by considering the computational time that will increase with the addition of contact formulation due to the high number of elements and nodes.

© 2024 The Authors. Advanced Engineering Materials published by Wiley-VCH GmbH

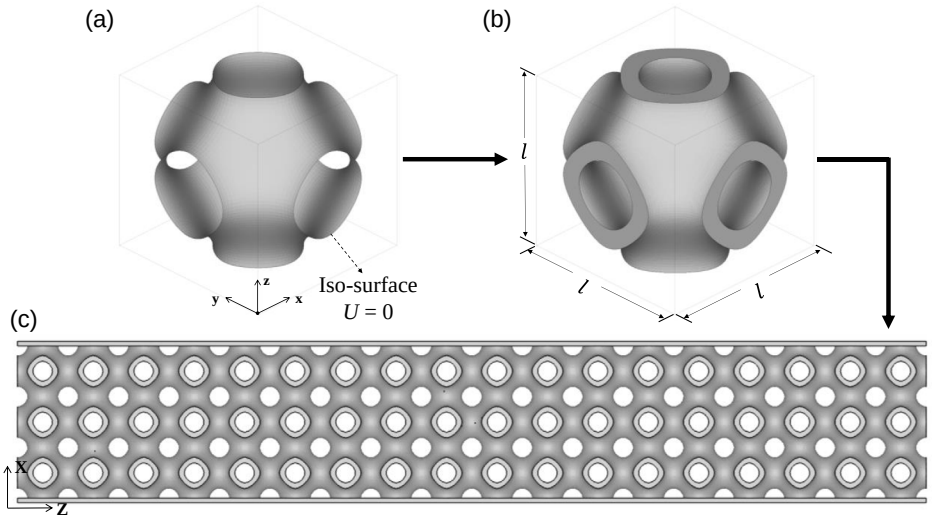

Figure 1. Primitive lattice's a) isosurface, b) unit cell with relative density $\rho^* = 0.2$, and c) fabricated structure.

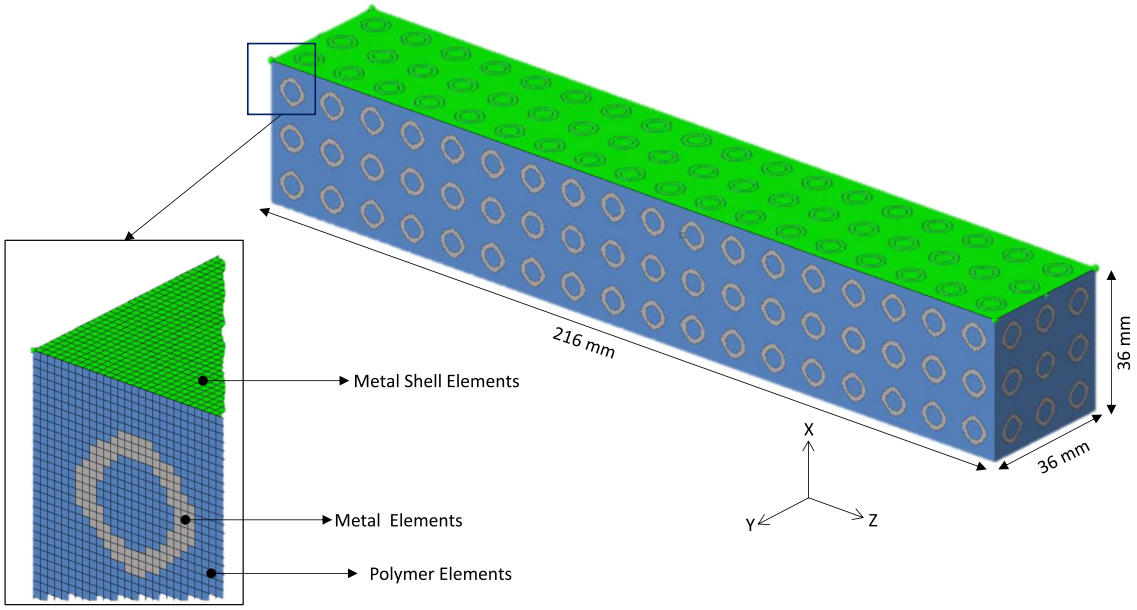

Figure 2. FEM model of hybrid structure.

Given that the examination of the hybrid structure's impact on damping capacity relative to the metal structure falls within the scope of this study, the nonlinear influences of preload and boundary conditions were excluded from the analyses. Therefore, FEM modeling was conducted under free-free conditions without any preload or boundary conditions. The material properties, shown in **Table 1**, are used in the FEM model.[24]

Table 1. Material properties used in the FEM model.

Material	Elastic modulus [GPa]	Poisson's ratio	Density [g cm^{-3}]
CoCr	236	0.33	8.3
Silicone	0.03	0.47	1.1

2.3. Polymer Material Selection

Material selection was predicated on a triad of selection criteria. The primary criterion is the density of the material, with emphasis on its minimization to ensure that weight efficacy of the emergent structure remains unencumbered. Subsequently, the mechanical loss coefficient served as the second determinant, elucidating the material's intrinsic vibration attenuation attributes. The mechanical loss coefficient or damping coefficient,

 © 2024 The Authors. Advanced Engineering Materials published by Wiley-VCH GmbH

15272648, 2024, 11, Downloaded from https://advanced.onlinelibrary.wiley.com/doi/10.1002/adem.202302181 by Ozyegin University, Wiley Online Library on [25/06/2025]. See the Terms and Conditions (https://onlinelibrary.wiley.com/terms-and-conditions) on Wiley Online Library for rules of use; OA articles are governed by the applicable Creative Commons License

η, is the measurement of the absorption of vibrational energy of a material. The damping coefficient is related to the dissipated energy and elastic energy of the structure when loaded.

In the pursuit of constructing a hybrid structure via the integration of a polymer layer, the optimal criterion would be to select a polymer that exhibits an elevated tan δ value. Tan δ, also known as the mechanical loss coefficient, is a term used to measure the mechanical damping properties of a material. It quantifies the energy dissipation due to the inelastic behavior of the material. Tan δ has several additional characteristics that allow a more comprehensive evaluation of its mechanical properties, temperature and frequency. These parameters play a pivotal role in shaping the mechanical behavior of viscoelastic materials, particularly influencing their damping characteristics. Consequently, tan δ emerges as a crucial analysis parameter for assessing the damping properties of polymer materials.[25]

The final criterion is the acoustic velocity, which refers to the propagation speed of an acoustic wave within a given medium. The medium's impedance invariably modulates the sound transmission, leading to energy dissipation. This metric elucidates the anticipated acoustic isolation proficiency of the prospective polymer selection. A correlation may exist between the acoustic isolation of a material and its vibration-damping capacities. Including acoustic velocity as a selection metric also augments the foresight into the hybrid structure's applicability in prospective acoustic investigations.

The selection of the material was rigorously predicated upon the aforementioned attributes. For this endeavor, we consulted the comprehensive material repository in Ansys GRANTA Research Selector.[25] Polymers, encompassing categories such as composites, elastomers, foams, and plastics, were evaluated as potential candidates for the augmentation of the hybrid structure. A plot showing the mechanical loss factor against density for these materials is illustrated in **Figure 3**. The material would exhibit a combination of minimum density and increased mechanical loss coefficient. The graphical representation reveals the supremacy of low-modulus silicone material in this realm. Complementarily, a criterion visualized through the acoustic velocity–density plot is elucidated in **Figure 4**. The silicone-based materials assumed a desired locus in this density–acoustic velocity matrix, representing the attributes of low-density and attenuated acoustic velocity. Synthesizing these selection frameworks, notably the high tan δ and diminished acoustic velocity attributes, the silicone-based compounds were identified as preeminent, driven by their intrinsic compatibility characteristics.

2.4. Damping Characterization Methods

Determining the damping properties is an important step in understanding the vibration characteristics of structural systems. The half-power bandwidth method (HPBW) is a simple method for fast and accurate calculation of modal damping ratios. It can also determine differences in damping ratios between different modes in a structure .[26]

The HPBW method was used to determine the half-power points in the frequency spectrum around a natural frequency. The HPBW is calculated by comparing the frequency range between the two points where the power is reduced to half in comparison to the amplitude at the natural frequency (see **Figure 5**). The HPBW of a mode is the frequency difference between its half-power points.[27]

Once HPBW is calculated, the modal damping ratio can be determined as the ratio between the HPBW and the natural frequency (ω_n), as given in Equation (3).

$$\zeta = \frac{\omega_2 - \omega_1}{\omega_n} \tag{3}$$

Intrinsically, a reciprocal relationship exists between the HPBW and the quality factor (Q-factor): a pronounced, high Q-factor indicates a system with a sharply delineated resonance peak, suggestive of low damping, while a decreasing Q-factor corresponds to a broader resonance spectrum, indicative of augmented damping.[28] Concurrently, the damping ratio (ζ) is given by Equation (4).

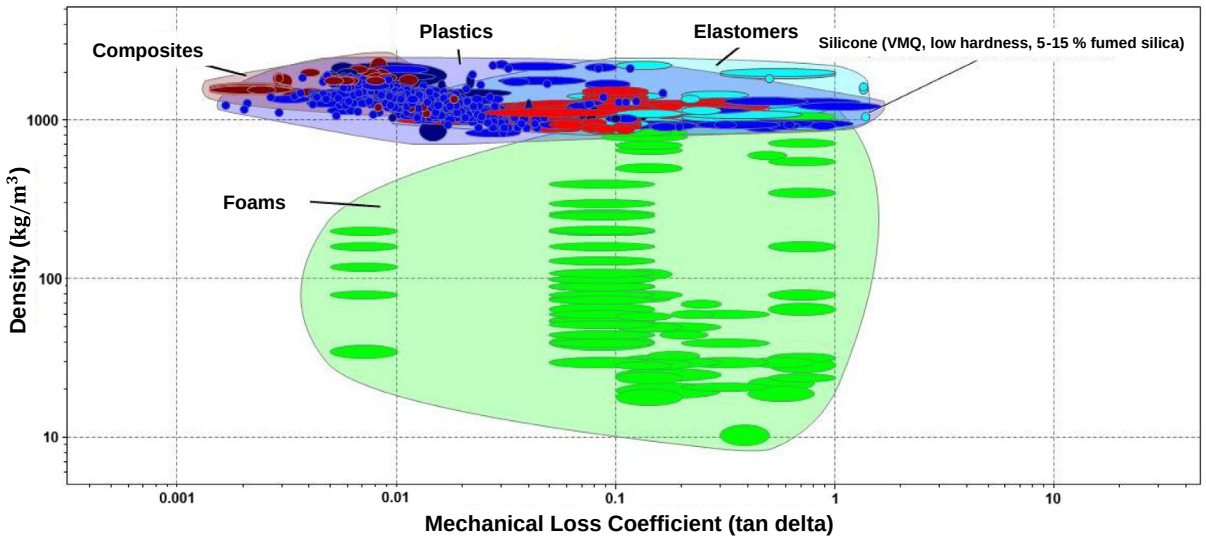

Figure 3. Density–mechanical loss coefficient graph.

© 2024 The Authors. Advanced Engineering Materials published by Wiley-VCH GmbH

15272648, 2024, 11, Downloaded from https://advanced.onlinelibrary.wiley.com/doi/10.1002/adem.202302181 by Ozyegin University, Wiley Online Library on [25/06/2025]. See the Terms and Conditions (https://onlinelibrary.wiley.com/terms-and-conditions) on Wiley Online Library for rules of use; OA articles are governed by the applicable Creative Commons License

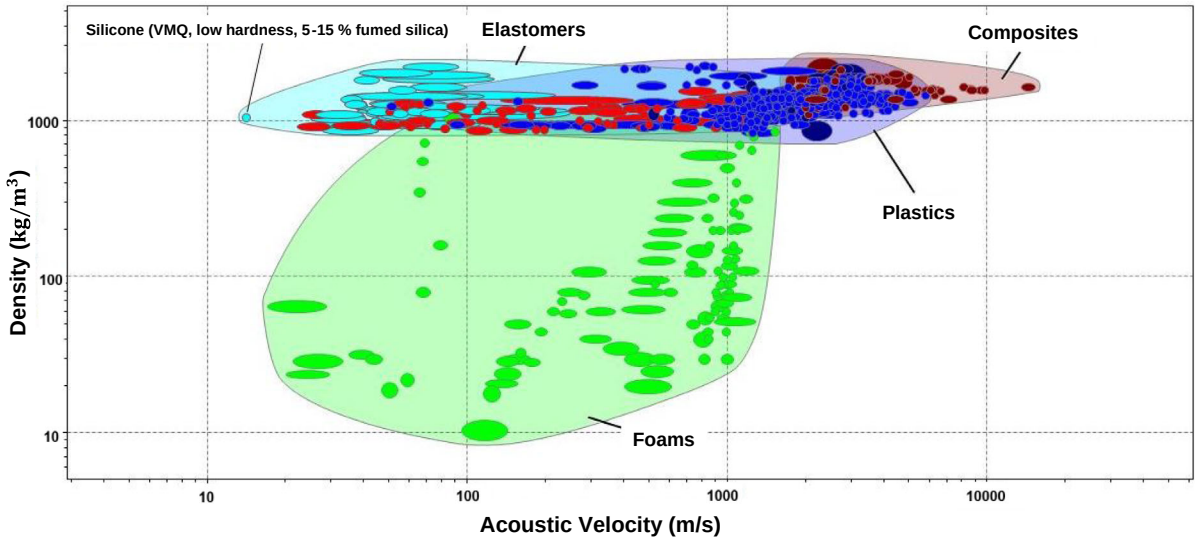

Figure 4. Density–acoustic velocity graph.

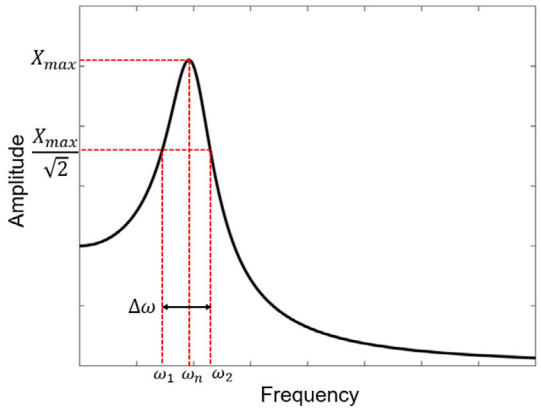

Figure 5. HPBW method for damping.

$$\zeta = \frac{1}{2Q} \tag{4}$$

In certain instances, *Q*-factor analysis may prove inefficient, particularly when applied to closely spaced resonant peaks, resulting in unreliable outcomes. The inefficiency arises from the proximity of the half-power points selected as the calculation parameter.[29] In light of the inefficiency observed with the *Q*-factor at resonance peaks in close proximity, we analyzed the test data using the Nyquist method under these conditions. The Nyquist method leverages phase information as well as the amplitude parameter to ascertain modal damping. This characteristic renders the method effective in characterizing damping even when dealing with resonance peaks in close proximity. The distinct phase behavior associated with each modal resonance facilitates the determination of modal characteristics and damping, enhancing the method's efficiency.[29]

The Nyquist method determines damping using the angles derived from the circle fit method applied to the resonance

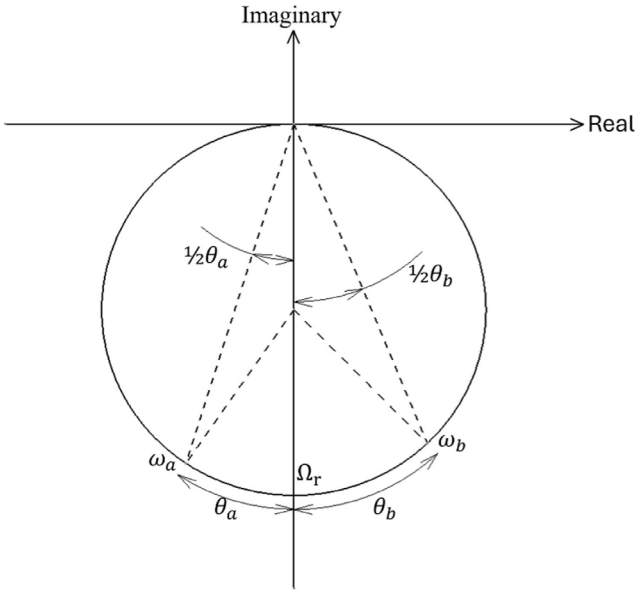

Figure 6. Nyquist diagram parameters.

and the two frequencies closest to this resonance frequency. The parameters of a sample Nyquist diagram are shown in **Figure 6**. The damping ratio, ζ_{ND}, is given in Equation (5).

$$\zeta_{ND} = 2 \cdot \frac{\omega_a - \omega_b}{\Omega_r \cdot (\tan(\theta_a/2) + \tan(\theta_b/2))} \tag{5}$$

where ζ_{ND} denotes the damping ratio, Ω_r denotes the resonance peak, and ω_a and ω_b represent the two frequency values proximate to this peak.

In the frequency-based analysis, the root sum of squares (RSS) of the overall accelerance function was used to compare the vibration behavior of the metal and hybrid parts with a single value.

© 2024 The Authors. Advanced Engineering Materials published by Wiley-VCH GmbH

15272648, 2024, 11, Downloaded from https://advanced.onlinelibrary.wiley.com/doi/10.1002/adem.202302181 by Ozyegin University, Wiley Online Library on [25/06/2025]. See the Terms and Conditions (https://onlinelibrary.wiley.com/terms-and-conditions) on Wiley Online Library for rules of use; OA articles are governed by the applicable Creative Commons License

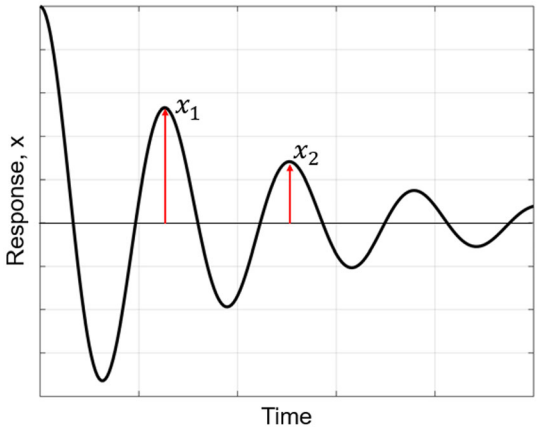

Figure 7. Logarithmic decrement technique parameters.

In addition to frequency domain analysis, damping characteristics were analyzed using logarithmic decrement method in time domain. Logarithmic decrement, $\overline{\zeta}$, is the natural logarithm of the amplitude ratio between two consecutive peaks (x_1, x_2) (see **Figure 7**).[30]

where x_1 represents the first amplitude peak and x_2 is the second amplitude peak. The damping ratio, ξ, is then calculated using Equation (6).

$$\xi = \frac{1}{\sqrt{1 + \left(\frac{2\pi}{\overline{\zeta}}\right)^2}} \tag{6}$$

In the present study, three distinct damping coefficients - the Q-factor, and Nyquist diagram damping ratio and the logarithmic decrement damping ratio were considered. The synergistic interpretation of these damping facilitates an exhaustive exploration of damping behavior across both frequency and time domains. Additionally, collecting these metrics from a variety of experimental methodologies bolsters the robustness and repeatability of the study, increasing the completeness and comprehensiveness of the findings obtained.

3. Fabrication and Experimental Validation

In this section, comprehensive FEM analyses are presented, along with the finalized design details obtained from these analyses, the production methodologies employed for fabricating the test specimens, and culminating verification studies with corresponding modal test outcomes.

3.1. FEM Analysis

The mesh strategy used in the FEM analysis performed in this study ensured an accurate representation of both the metallic and polymer regions of the TPMS structure. Following the modal analysis, harmonic analysis was performed to obtain frequency response function (FRF) data for metal and hybrid structures. The related FRF data were generated separately for each response axis and are presented on a single graph. The obtained analysis results were consistent with the observed experimental modal test findings and further strengthened the accuracy and robustness of the FEM model. The FRF results in **Figure 8** show the transition of modal frequencies toward lower values. The analysis simulations also provided valuable insights into potential design modifications that could further exploit the combined potential of the TPMS additive metal and silicone polymer to achieve an even higher damping performance.

The mode shapes obtained from the modal analysis are presented in **Figure 9** and show parallelism for hybrid and metal structures.

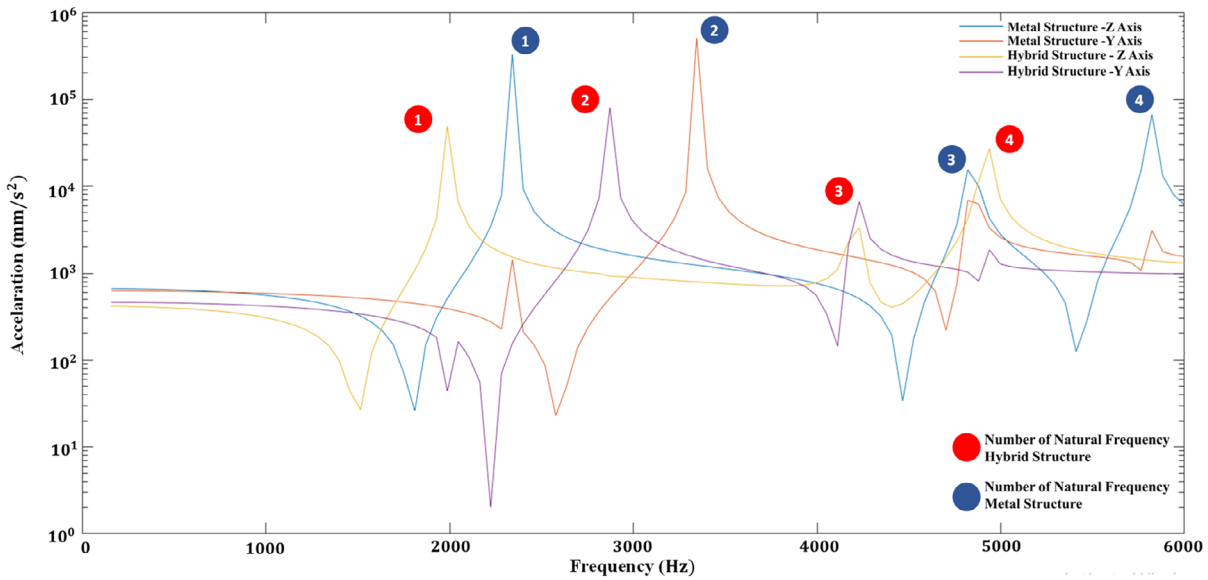

Figure 8. Acceleration FRFs of FEM analysis.

© 2024 The Authors. Advanced Engineering Materials published by Wiley-VCH GmbH

15272648, 2024, 11, Downloaded from https://advanced.onlinelibrary.wiley.com/doi/10.1002/adem.202302181 by Ozyegin University, Wiley Online Library on [25/06/2025]. See the Terms and Conditions (https://onlinelibrary.wiley.com/terms-and-conditions) on Wiley Online Library for rules of use; OA articles are governed by the applicable Creative Commons License

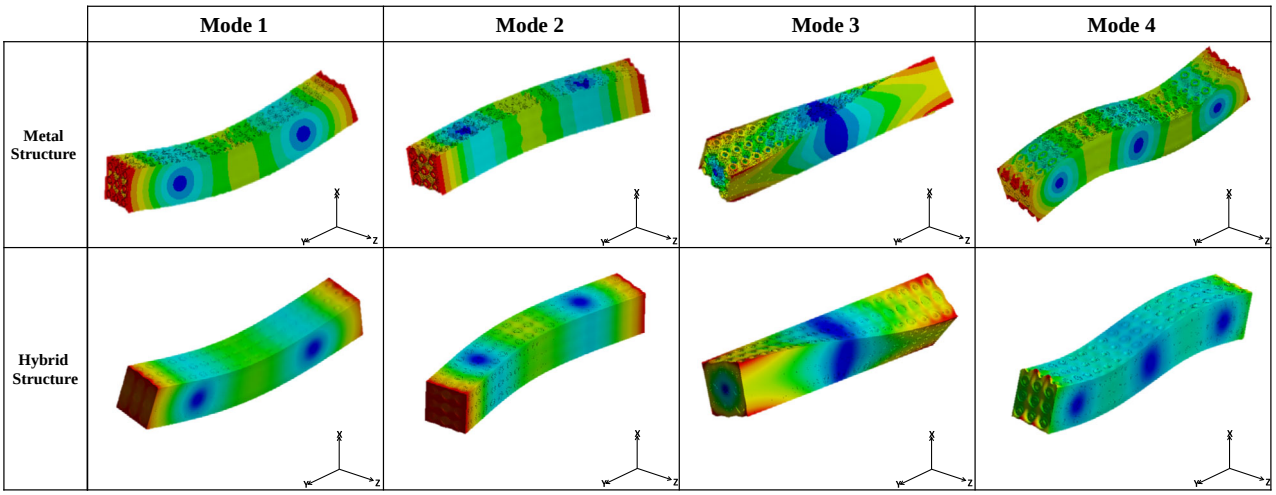

Figure 9. Mode shapes from FEM analysis.

3.2. Manufacturing Process of Test Specimen

In this study, a CoCr test specimen filled with primitive lattices was printed using LPBF technology. Breakaway supports were used between the lattice part and the build plate to minimize distortions, which may occur due to high thermal gradients and cause a build failure. The contact surface area between support structures and the lattice part was optimized to enable their simple removal without sacrificing its main functionality.[31]

For the fabrication phase (see **Figure 10**), the build data, encoded in a machine-interpretable format, was inputted into a Concept Laser M2 Cusing system. The powder chamber was loaded with a spherical CoCr powder, characterized by a particle size distribution ranging from 10 to 45 μm. The Laser Powder Bed Fusion (LPBF) process parameters were carefully calibrated, setting the layer thickness at 50 μm, utilizing a laser power setting of 180 W, a scanning speed of 1500 mm s^{-1}, and a hatch spacing of 60 μm, all under a controlled argon atmosphere. The production was carried out on a build plate made of carbon steel, with 100 °C as preheating.[31,32] After the LPBF process, the residual powder particles adhering to the specimens were removed via the SFM-AT800 system. The delineation of the specimens from the build plate was conducted using wire electrical discharge machining. This was followed by the manual detachment of the breakaway support structures.[33]

The voids in the metal structure were filled using liquid silicone mixed with a curing activator. More specifically, a 5-shore translucent silicone with a commercial name of RTV 3005 was mixed with a commercial type of catalyst called RTV-3000 at a ratio of 2%. The mixture was then slowly applied in liquid form to the voids of the TPMS metal structure. The desired hybrid structure was obtained after a 24 h curing time at room temperature. Ensuring the exhaustive occupancy of the voids was meticulously gauged via a combination of the known density of the polymer and stringent control over the cavity volume. Employing this methodology, the aggregate weight of the hybrid structure postvoid filling was compared to a theoretical weight, derived from the established density of the silicone polymer and the designated fill volume.

3.3. Modal Test and Validation

Modal testing is an experimental method used to determine the natural frequencies and associated mode shapes of structural systems. In general, this method encompasses three primary steps: excitation, measurement, and postprocessing of the results. In this process, structures are typically excited with impact hammers or shakers. Then, the vibration response of the structural system is measured using accelerometers. Finally, the data

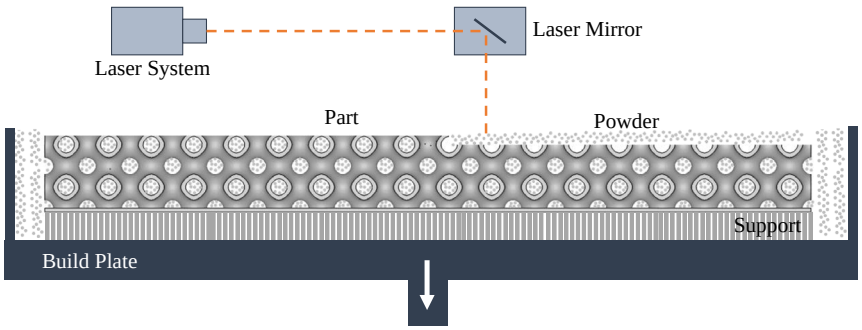

Figure 10. Schematic of the additive manufacturing process of the lattice structure.

© 2024 The Authors. Advanced Engineering Materials published by Wiley-VCH GmbH

15272648, 2024, 11, Downloaded from https://advanced.onlinelibrary.wiley.com/doi/10.1002/adem.202302181 by Ozyegin University, Wiley Online Library on [25/06/2025]. See the Terms and Conditions (https://onlinelibrary.wiley.com/terms-and-conditions) on Wiley Online Library for rules of use; OA articles are governed by the applicable Creative Commons License

collected is postprocessed to determine the natural frequencies and mode shapes of the structural system. In this study, a modal analysis was conducted utilizing an impact hammer and an accelerometer to determine the natural frequencies and mode shapes of metallic and hybrid structural systems.

Particularly, the transfer function between the excitation force and acceleration response data of the test piece was analyzed. The transfer function between the measured acceleration and the force is known as the accelerance of the frequency response.

In modal testing, the test specimen is placed on PU foam to simulate a free-free structure with no initial conditions such as boundary conditions or preloads, for the test piece. DEWESoft hardware and software were used for data acquisition and processing of the modal test results in modal tests. The analog signals are converted to digital signals using DEWESoft Sirius hardware. An MMF brand accelerometer with a sensitivity of 102 mV g^{-1} and a DJB brand impact hammer with a sensitivity of 2.5 mV N^{-1} was used for the test equipment. The modal test setup is shown in **Figure 11**.

A modal test was conducted using the multiple input single output method. The acceleration data is collected from a single point from the accelerometer while the impact hammer excites the structure from five different locations. These locations are marked on the test specimen, as shown in Figure 11.

The accelerance frequency response results from modal testing are shown for metal and hybrid structures in **Figure 12**. The amplitude of the accelerance is given in dB. The peak points in the transfer function represent the natural frequency points of this structure.

The modal analysis revealed marked distinctions between the dynamic characteristics of the metal and hybrid structures. Of the two methods applied to modal test results, HPBW and Nyquist diagrams were generated from the modal test results of both metal and hybrid structures to determine the damping values of each resonance peak. The resulting damping values and Q-factors are shown in **Table 2**. When the damping ratios are examined, it is seen that while the damping ratios are 0.001 in the first four modes of the metal structure, these ratios increase to 0.068 and 0.063 in the first and second modes and 0.042 for the third and fourth modes in the hybrid structure.

It was determined from the RSS analysis that the vibration response of the metal structure to the overall acceleration was reduced by 90% when the RSS data derived from acceleration was compared with the accelerometer data.

The incorporation of hybrid materials seems to have bolstered the energy dissipation capabilities, altering the intrinsic vibrational characteristics. This highlights the pivotal role of material hybridization in tailoring and potentially enhancing the vibrational response of structures.

The damping characteristic tests in the time domain of our research focused on the damping over time of a pulse of similar amplitude generated in the test pieces. The impacts were obtained with a modal hammer, impact amplitudes were kept within the same limits, and the test pieces were tested under the same test conditions. When analyzing the damping characteristics, we extracted two main aspects: the logarithmic decrease of the vibration due to impact and subsequent damping ratios and the energy damping time in **Figure 13**. We further characterized the overall damping behavior using the damping ratio obtained from logarithmic decrement as a benchmark. The hybrid structure exhibited a fast-damping capacity, neutralizing

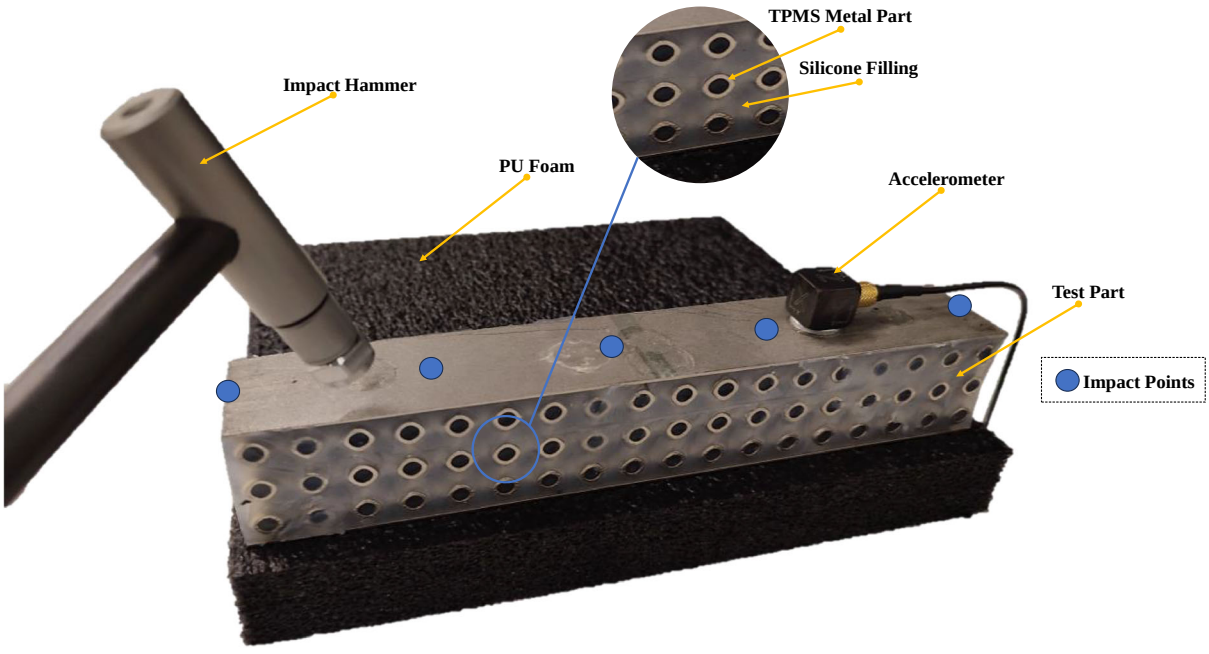

Figure 11. Modal test setup.

© 2024 The Authors. Advanced Engineering Materials published by Wiley-VCH GmbH

15272648, 2024, 11, Downloaded from https://advanced.onlinelibrary.wiley.com/doi/10.1002/adem.202302181 by Ozyegin University, Wiley Online Library on [25/06/2025]. See the Terms and Conditions (https://onlinelibrary.wiley.com/terms-and-conditions) on Wiley Online Library for rules of use; OA articles are governed by the applicable Creative Commons License

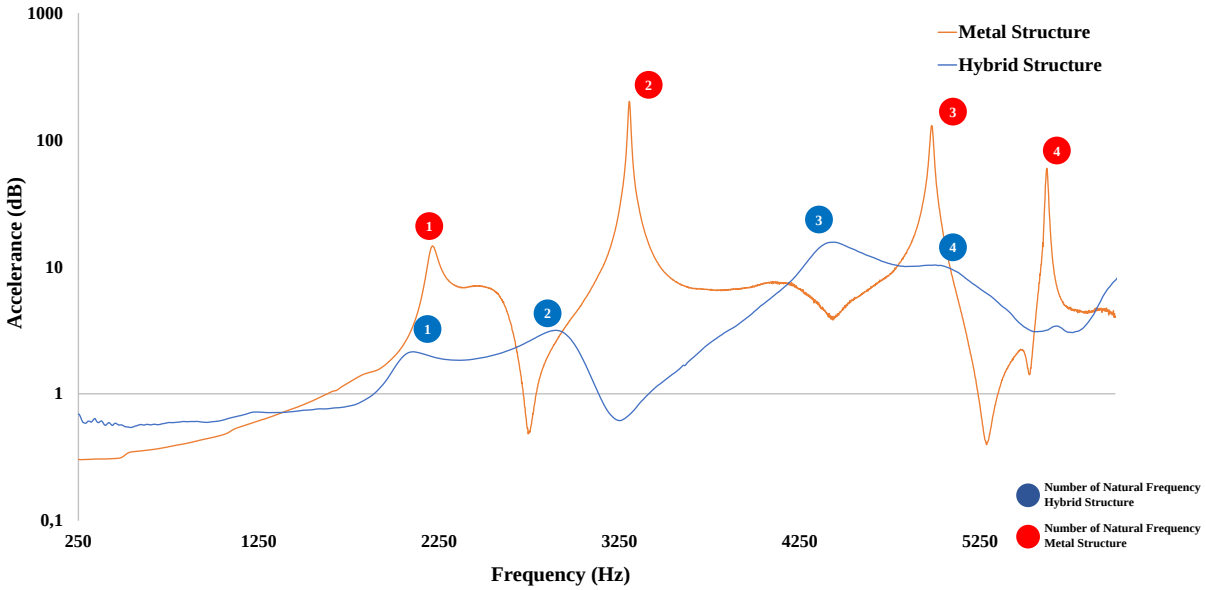

Figure 12. Comparison of the test results in terms of accelerance: hybrid versus metal parts.

Table 2. Modal test results.

Test part	Frequency [Hz]	HPBW Q-factor	Nyquist diagram damping ratio (ζ_{ND})
Metal	2212	78.5	0.001
	3304	220.6	0.002
	4981	237.4	0.001
	5623	294.8	0.001
Hybrid	2041	2.3	0.068
	2958	7.6	0.063
	4443	10.8	0.042
	4961	4.5	0.042

the vibrations in just 0.005 s, which is the reference data of the damping coefficients obtained by logarithmic decrement. In parallel, we also took into account the time required to absorb the impact energy, providing a holistic view of how quickly the effects of the impact dissipate. The data obtained are presented in **Table 3**.

The in-depth time domain analysis highlighted the superior damping capabilities of the hybrid structure. Using both the logarithmic damping ratio and the duration for energy dissipation as key indicators, the performance of the hybrid structure to mitigate the vibrations from an external impact became evident. The rapidity with which it neutralizes vibrations, in merely 0.005 s, offers compelling evidence of its robust damping potential. Moreover, the concurrent consideration of the energy absorption time frame enriches our understanding of the hybrid structure's performance to minimize the effects of an impact.

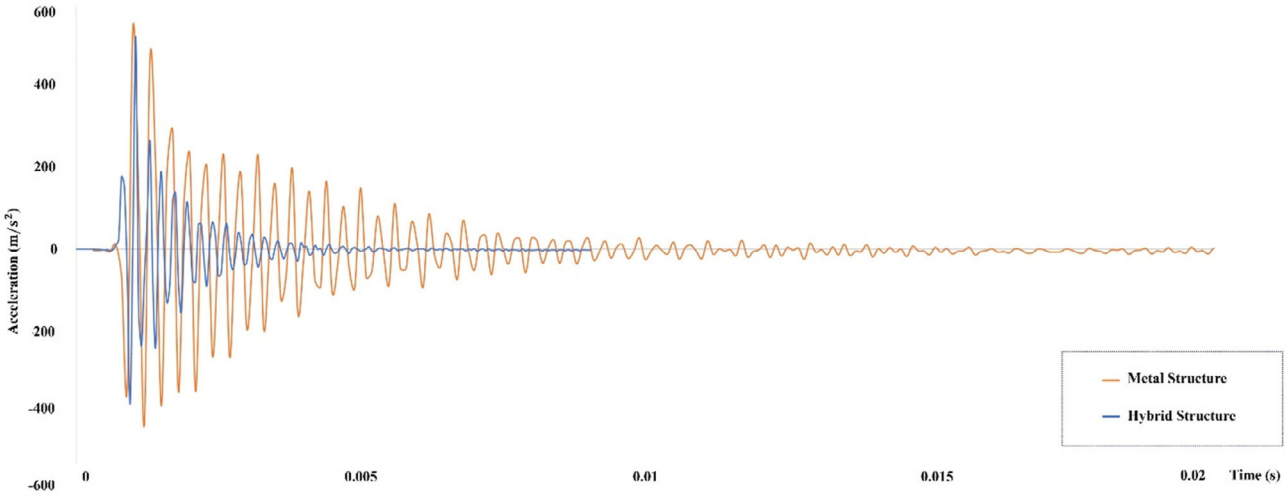

Figure 13. Acceleration versus time history.

© 2024 The Authors. Advanced Engineering Materials published by Wiley-VCH GmbH

15272648, 2024, 11, Downloaded from https://advanced.onlinelibrary.wiley.com/doi/10.1002/adem.202302181 by Ozyegin University, Wiley Online Library on [25/06/2025]. See the Terms and Conditions (https://onlinelibrary.wiley.com/terms-and-conditions) on Wiley Online Library for rules of use; OA articles are governed by the applicable Creative Commons License

Table 3. Damping ratio (ξ) and settling time.

Test part	Damping ratio [ξ]	Settling time [s]
Metal	0.12	0.04
Hybrid	0.80	0.005

Table 4. Comparison of FEM and experimental results.

		Test results [Hz]	FEM results [Hz]	% Rel. error [%]
Metal structure	1. Mode	2212	2340	6
	2. Mode	3304	3358	2
	3. Mode	4981	4841	3
	4. Mode	5623	5810	3
Hybrid structure	1. Mode	2041	1994	2
	2. Mode	2958	2867	3
	3. Mode	4443	4208	5
	4. Mode	4961	4918	1

4. Discussion

The precision achieved in modeling, with a maximum error of only 6% in both testing and FEM analyses, reinforces the reliability and accuracy of the established FEM models. Upon scrutinizing the FEA outcomes, which closely align with experimental data exhibiting minimal discrepancies shown in **Table 4**, the enhanced damping potential of the hybrid structure reinforced by the polymer material becomes evident. This is manifestly reflected in the frequency shifts and attenuation in amplitude discerned within the FRF plots. Furthermore, a comparative assessment of the mode shapes for both the metal and hybrid structures reveals a noteworthy observation: the presence of the polymer does not perturb the mode shapes, ensuring consistent mode shapes across both entities.

From the perspective of time-domain analysis and considering the RSS analysis, it is evident that the hybrid structure demonstrates superior damping characteristics compared to the metallic structure. The analyses of the experimental results were carried out by more than one method within the framework of HPBW and Nyquist diagrams. As the Q factor values obtained from the HPBW method proved inefficient in cases where two resonances closely coexisted, the analyses were extended using the Nyquist method. According to the Q factor values, an increase in damping ranging from 20% to 27% was observed for the first three modes, while the fourth mode exhibits a damping ratio of ≈50%. This increase is attributed to the proximity of the third and fourth modes. On the contrary, when the damping values obtained from the Nyquist method are examined, it is seen that while damping ratios are recorded as 0.001 in the first four modes of the metal structure, these ratios increase to 0.068 and 0.063 for the first and second modes and 0.042 for the third and fourth modes in the hybrid structure.

The efficiency of the metal–polymer contacts utilized in the FEM modeling of the hybrid structure is effective for the first four natural frequencies; however, their effectiveness at higher frequencies warrants extra analysis. Furthermore, investigating the efficiency of this hybrid structure in different TPMS structures and diverse metal–polymer combinations is critically important for expanding the impact of the findings of this study.

Cumulatively, these insights confirm the hypothesis that the FEM framework accurately captures the increased damping efficiency inherent to the hybrid structure, thereby reaffirming the model's predictive fidelity. By analyzing the results in both frequency and time domains, it was evident that enhanced damping performance was achieved, especially noticeable in the reduction of vibration amplitude.

5. Conclusion

In conclusion, this study has showcased the promising potential of TPMS additive metal parts combined with silicone polymer in revolutionizing damping properties for various engineering applications. Insights from FEM modeling, complemented by experimental modal testing, have established a robust synergy between metal and polymer material, leading to significant advancements in damping characteristics.

The key findings of this study pertain to frequency and time-domain damping analyses. The hybrid structure significantly improves the damping characteristics according to the results of HPBW, Nyquist, and logarithmic decrement methods. Furthermore, the overall accelerance values obtained from frequency-based analyses represent another significant outcome, showcasing a tenfold reduction in RSS data. This reduction serves as an additional indicator of the hybrid structure's ability to enhance the system's damping capacity under dynamic loads.

The findings from this study suggest that the hybrid structure can be pivotal in applications related to vibration damping and acoustics. The vibration-damping proficiency exhibited by hybrid architecture from this research undeniably positions it as a paradigm for subsequent scientific inquiries aiming to harness its inherent potentialities, especially in acoustic isolation systems. As such, it offers a foundational reference for various studies aiming to use these hybrid structures in these domains. As the field of materials science continues to evolve, the insights from this study pave the way for future endeavors, aiming to harness the optimal benefits of hybrid structures in addressing critical damping and acoustic challenges across various engineering spectra.

Acknowledgements

The authors acknowledge the support provided by Ansys GRANTA Research Selector and Onatus for providing an evaluation license and facilitating the use of Ansys GRANTA Research Selector.

Conflict of Interest

The authors declare that they have no conflict of interest.

© 2024 The Authors. Advanced Engineering Materials published by Wiley-VCH GmbH

15272648, 2024, 11, Downloaded from https://advanced.onlinelibrary.wiley.com/doi/10.1002/adem.202302181 by Ozyegin University, Wiley Online Library on [25/06/2025]. See the Terms and Conditions (https://onlinelibrary.wiley.com/terms-and-conditions) on Wiley Online Library for rules of use; OA articles are governed by the applicable Creative Commons License

Data Availability Statement

The data that support the findings of this study are available from the corresponding author upon reasonable request.

Keywords

damping hybrid structures, modal testing, silicone polymers, triply periodic minimal surface lattices

Received: December 19, 2023
Revised: March 29, 2024
Published online: May 2, 2024

[1] J. Fan, L. Zhang, S. Wei, Z. Zhang, S. K. Choi, B. Song, Y. Shi, *Mater. Today* **2021**, *50*, 303.
[2] K. Monkova, M. Vasina, M. Zaludek, P. P. Monka, J. Tkac, *Materials* **2021**, *14*, 1502.
[3] R. Rajpal, K. P. Lijesh, K. V. Gangadharan, *Addit. Manuf.* **2018**, *22*, 583.
[4] A. Abusabir, M. A. Khan, M. Asif, K. A. Khan, *Polymers* **2022**, *14*, 618.
[5] Z. Xu, C. S. Ha, R. Kadam, J. Lindahl, S. Kim, H. F. Wu, V. Kunc, X. Zheng, *Addit. Manuf.* **2020**, *32*, 101106.
[6] W. Elmadih, W. P. Syam, I. Maskery, D. Chronopoulos, R. Leach, *Addit. Manuf.* **2019**, *25*, 421.
[7] J. Zhang, Y. Shen, Y. Sun, J. Yang, Y. Gong, K. Wang, Z. Zhang, X. Chen, L. Bai, *J. Mater. Res. Technol.* **2022**, *18*, 3240.
[8] M. J. Prajapati, A. Kumar, S. C. Lin, J. Y. Jeng, *Addit. Manuf.* **2022**, *54*, 102766.
[9] T. Ehlers, S. Tatzko, J. Wallaschek, R. Lachmayer, *Addit. Manuf.* **2021**, *38*, 101752.
[10] H. Guo, K. Ichikawa, H. Sakai, H. Zhang, X. Zhang, K. Tsuruta, K. Makihara, A. Takezawa, *Powder Technol.* **2022**, *396*, 696.
[11] B. C. Chakraborty, D. Ratna, *Polymers for Vibration Damping Applications*, Elsevier, Amsterdam **2020**.
[12] P. S. Badkar, M. M. Benal, *Mater. Today: Proc.*, **2022**, *59*, 679.
[13] L. Yu, S. Liu, L. Ye, G. Huang, Y. Xu, *J. Wuhan Univ. Technol., Mater. Sci. Ed.*, **2012**, *27*, 130.
[14] C. Zhang, K. Pal, J. U. Byeon, S. M. Han, J. K. Kim, *J. Appl. Polym. Sci.* **2011**, *119*, 2737.
[15] Y. Liu, Z. Liu, Q. Song, B. Wang, *J. Mater. Process. Technol.* **2019**, *266*, 687.
[16] Z. Fang, L. Yao, J. Hou, Y. Xiao, *Materials* **2022**, *15*, 3512.
[17] A. S. Dalaq, D. W. Abueidda, R. K. Abu Al-Rub, I. M. Jasiuk, *Int. J. Solids Struct.* **2016**, *83*, 169.
[18] I. Hussain, O. Al-Ketan, F. Renda, M. Malvezzi, D. Prattichizzo, L. Seneviratne, R. K. Abu Al-Rub, D. Gan, *Int. J. Rob. Res.* **2020**, *39*, 1635.
[19] A. Singh, O. Al-Ketan, N. Karathanasopoulos, *Composites, Part B* **2023**, *251*, 110478.
[20] X. Guo, J. Ding, X. Li, S. Qu, J. Y. H. Fuh, W. F. Lu, X. Song, W. Zhai, *Composites, Part B* **2023**, *248*, 110351.
[21] E. D. Betters, J. West, M. Noakes, A. Nycz, S. Smith, T. L. Schmitz, *Precis. Eng.* **2020**, *66*, 125.
[22] R. Wang, Y. Chen, X. Peng, N. Cong, D. Fang, X. Liang, J. Shang, *Rapid Prototyping J.* **2022**, *28*, 1995.
[23] M. Ozdemir, U. Simsek, E. Kuser, C. E. Gayir, A. Celik, P. Sendur, *Adv. Eng. Mater.* **2023**, *25*, 2201811.
[24] U. Simsek, A. Akbulut, C. E. Gayir, C. Basaran, P. Sendur, *Int. J. Adv. Manuf. Technol.* **2021**, *115*, 657.
[25] *Ansys® GRANTA Research Selector, Release 2023 R2*, ANSYS, Inc., USA **2023**.
[26] D. J. Ewins, *Modal Testing: Theory, Practice and Application*, John Wiley & Sons, London **2009**.
[27] J. S. Bendat, A. G. Piersol, *Random Data: Analysis and Measurement Procedures*. John Wiley & Sons, California **2011**.
[28] B. Singh, B. K. Nanda, *Shock Vibr.* **2012**, *19*, 1463.
[29] C. Beards, *Structural Vibration: Analysis and Damping*, Elsevier, MA **1996**.
[30] W. J. Bottega, *Engineering Vibrations*, CRC Press, Boca Raton, FL **2014**.
[31] S. L. Sing, S. Huang, W. Yee Yeong, *Mater. Sci. Eng., A* **2020**, *769*, 138511.
[32] B. AlMangour, D. G. Monis Luqman, H. Al-Harbi, F. Ijaz, *Mater. Sci. Eng., A* **2020**, *792*, 139456.
[33] M. Ozdemir, U. Simsek, G. Kiziltas, C. E. Gayir, A. Celik, P. Sendur, *Addit. Manuf.* **2023**, *70*, 103560.

© 2024 The Authors. Advanced Engineering Materials published by Wiley-VCH GmbH

15272648, 2024, 11, Downloaded from https://advanced.onlinelibrary.wiley.com/doi/10.1002/adem.202302181 by Ozyegin University, Wiley Online Library on [25/06/2025]. See the Terms and Conditions (https://onlinelibrary.wiley.com/terms-and-conditions) on Wiley Online Library for rules of use; OA articles are governed by the applicable Creative Commons License